

Blood Gene Expression Profile Study Revealed the Activation of Apoptosis and p53 Signaling Pathway May Be the Potential Molecular Mechanisms of Ionizing Radiation Damage and Radiation-Induced Bystander Effects

Dose-Response:
An International Journal
January-March 2020:1-11
© The Author(s) 2020
Article reuse guidelines:
sagepub.com/journals-permissions
DOI: 10.1177/1559325820914184
journals.sagepub.com/home/dos



Guangyao He¹, Anzhou Tang¹, Mao Xie¹, Wei Xia¹, Pengcheng Zhao¹, Jianglian Wei¹, Yongjing Lai¹, Xianglong Tang¹, Yi Ming Zou² , and Heng Liu³

Abstract

Radiotherapy is an effective treatment for local solid tumors, but the mechanism of damage to human body caused by radiation therapy needs further study. In this study, gene expression profiles of human peripheral blood samples exposed to different doses and rates of ionizing radiation (IR) were used for bioinformatics analysis to investigate the mechanism of IR damage and radiation-induced bystander effect (RIBE). Differentially expressed genes analysis, weighted gene correlation network analysis, functional enrichment analysis, hypergeometric test, gene set enrichment analysis, and gene set variation analysis were applied to analyze the data. Moreover, receiver operating characteristic curve analysis was performed to identify core genes of IR damage. Weighted gene correlation network analysis identified 3 modules associated with IR damage, 2 were positively correlated and 1 was negatively correlated. The analysis showed that the positively correlated modules were significantly involved in apoptosis and p53 signaling pathway, and ESRI, ATM, and MYC were potential transcription factors regulating these modules. Thus, the study suggested that apoptosis and p53 signaling pathway may be the potential molecular mechanisms of IR damage and RIBE, which could be driven by ESRI, ATM, and MYC.

Keywords

ionizing radiation damage, radiation-induced bystander effect, transcription factor, WGCNA

Introduction

In the past 20 years, radiotherapy has become the primary cytotoxic therapy for localized solid cancer.¹ Radiotherapy using ionizing radiation (IR) to destroy cancer cells by irradiating cancerous tumors with high doses of radiation produced by special equipment, thus inhibiting their growth, reproduction, and proliferation.² However, IR has been shown to cause severe cell damage.³ Cells exposed to IR showed increased frequency of DNA damage, apoptosis, and chromosomal aberration or mutation. For a long time, it had been generally believed that these biological events are mainly caused by the action of reactive oxygen species formed by ionization and water irradiation of cell structure. Recently, however, attentions have been paid to the bystander effect.⁴ Radiation-induced bystander effect (RIBE) is induced by reagents and

¹ Department of Otolaryngology–Head and Neck Surgery, The First Affiliated Hospital of Guangxi Medical University, Nanning, Guangxi, China

² Department of Mathematical Sciences, University of Wisconsin-Milwaukee, Milwaukee, WI, USA

³ School of Information and Management, Guangxi Medical University, Nanning, Guangxi, China

Received 22 October 2019; received revised 04 February 2020; accepted 18 February 2020

Corresponding Authors:

Yi Ming Zou, Department of Mathematical Sciences, University of Wisconsin-Milwaukee, Milwaukee, WI 53201, USA.

Email: ymzou@uwm.edu

Heng Liu, School of Information and Management, Guangxi Medical University, Nanning, Guangxi 530021, China.

Email: liuheng@gxmu.edu.cn



Creative Commons Non Commercial CC BY-NC: This article is distributed under the terms of the Creative Commons Attribution-NonCommercial 4.0 License (<https://creativecommons.org/licenses/by-nc/4.0/>) which permits non-commercial use, reproduction and distribution of the work without further permission provided the original work is attributed as specified on the SAGE and Open Access pages (<https://us.sagepub.com/en-us/nam/open-access-at-sage>).

signals emitted by directly irradiated cells, which cause the lowering of survival, cytogenetic damage, apoptosis enhancement, and biochemical changes in neighboring nonirradiated cells.^{3,5} Endocrine molecules of irradiated tumor cells may cause damage to adjacent normal cells.⁶ Cells exposed to IR and other genotoxic agents (targeted cells) can communicate their DNA damage response (DDR) status to cells that have not been directly irradiated (bystander cells).⁷ Molecular signals can be transmitted through gap junction, intercellular communication, and mediator transfer mechanisms. However, the biological mechanism of this effect is still not well understood. Many studies have proposed to estimate the dose in irradiated peripheral blood based on gene expressions and showed that peripheral blood is capable of reflecting the degree of radiation exposure.⁸⁻¹¹ In addition, the irradiated tumor tissue contains many capillaries, and factors or biomarkers produced by irradiated tissue can enter the bloodstream through capillaries, though the radiation dosage is relatively small, it could induce RIBE. Therefore, we proposed to use gene expression profiles in peripheral blood to study bystander effects and IR loss, since the gene expression patterns of irradiated peripheral blood may provide information on the molecular mechanism of RIBE.

In our study, radiation-induced gene expression of peripheral blood at the 24-hour time point after irradiation was used to perform weighted correlation network analysis (WGCNA). The analysis showed that apoptosis and p53 signaling pathway (as the major Kyoto Encyclopedia of Genes and Genomes [KEGG] pathway of functional module) may be the potential mechanism of bystander effects and IR. In addition, strong changes were identified in gene expressions in both irradiated and nonirradiated cells by hypergeometric testing. We also found that 3 transcription factors (TFs; ESR1, ATM, and MYC) and their downstream target genes may play a central role in the biological response to IR. Subsequently, a TF-target genes pathway global regulatory network was constructed for the involved genes. Furthermore, our study also identified 13 core molecules that have the ability to distinguish radiation exposure from nonradiation exposure in peripheral blood.

Materials and Methods

Data Selection

Three data sets (GSE65292, GSE55953, and GSE212400) were found in the Gene Expression Omnibus (GEO) database by searching with the keywords “radiation” and “blood gene expression profiles.”

Data Processing

The human peripheral blood gene expression profiles of GSE65292¹² were downloaded from the GEO database (<https://www.ncbi.nlm.nih.gov/geo/>),¹³ which was based on GPL13497. The profiles contain 30 irradiated human whole blood samples and 5 normal controls. The doses (0.56, 2.2, and 4.45 Gy) were delivered by 2 dose rates, acute dose rate of 1.1

Gy/min and low-dose rate of 3.1 mGy/min. In addition, GSE55953^{14,15} based on GPL14550, including 8 IR samples and 20 normal controls, and GSE21240 based on GPL6480, including 24 IR samples and 24 controls, were used to validate the aberrant expressions of genes of interest. The *normalizeBetweenArrays* function in the *limma* package¹⁶ was used to normalize the gene expression profiles. If a gene responded to multiple probes, the average value of these probes was considered to be the expression value of the corresponding gene. The workflow of the study is shown in Figure 1.

Gene Set Enrichment Analysis and Gene Set Variation Analysis

Gene set enrichment analysis (GSEA) was performed using the normalized gene expression profiles to explore the biological process (BP) and KEGG pathways in relation with different dose- and rate-radiation damage. The Java software of GSEA (version 2-2.2.4) was used in the analysis. The *c5.bp.v6.2.symbols.gmt* and *c2.cp.kegg.v6.2.symbols.gmt* data sets in *MsigDB V6.2* database¹⁷ were used as reference gene sets, and GSEA was performed according to default parameters. $P < 0.05$ was considered significant. In addition, gene set variation analysis (GSVA) package¹⁸ in R was used to estimate the expression of the gene set in the individual samples.

Differentially Expressed Gene Analysis

Compared to the control samples, the differentially expressed genes (DEGs) in 0.56 Gy dose samples, 2.2 Gy dose samples, 4.45 Gy dose samples, 1.1 Gy/min rate samples, and 3.1-mGy/min rate samples were analyzed using the *limma* package in R. The genes with P adjusted by the false discovery rate $< .01$ were considered significant.

Weighted Gene Correlation Network Analysis in GSE65292

All DEGs of 5 comparisons in GSE65292 were extracted to perform WGCNA.¹⁹ First, *hclust* function was used for hierarchical clustering analysis. Then, the soft thresholding power value was screened during module construction by the *pickSoftThreshold* function. Candidate power (1-30) was used to test the average connectivity degrees of different modules and their independence. In the analysis, the power values were automatically estimated by WGCNA. The WGCNA R package was also used to construct coexpression networks (modules), where the minimum module size was set to 30 and each module was assigned a unique color label.

Functional Enrichment Analysis

To further explore the biological significance of the functional modules, Gene Ontology (GO) and KEGG pathway enrichment analyses for the module genes were performed, respectively, using the *clusterProfiler* package²⁰ in R. A $P < 0.05$ was

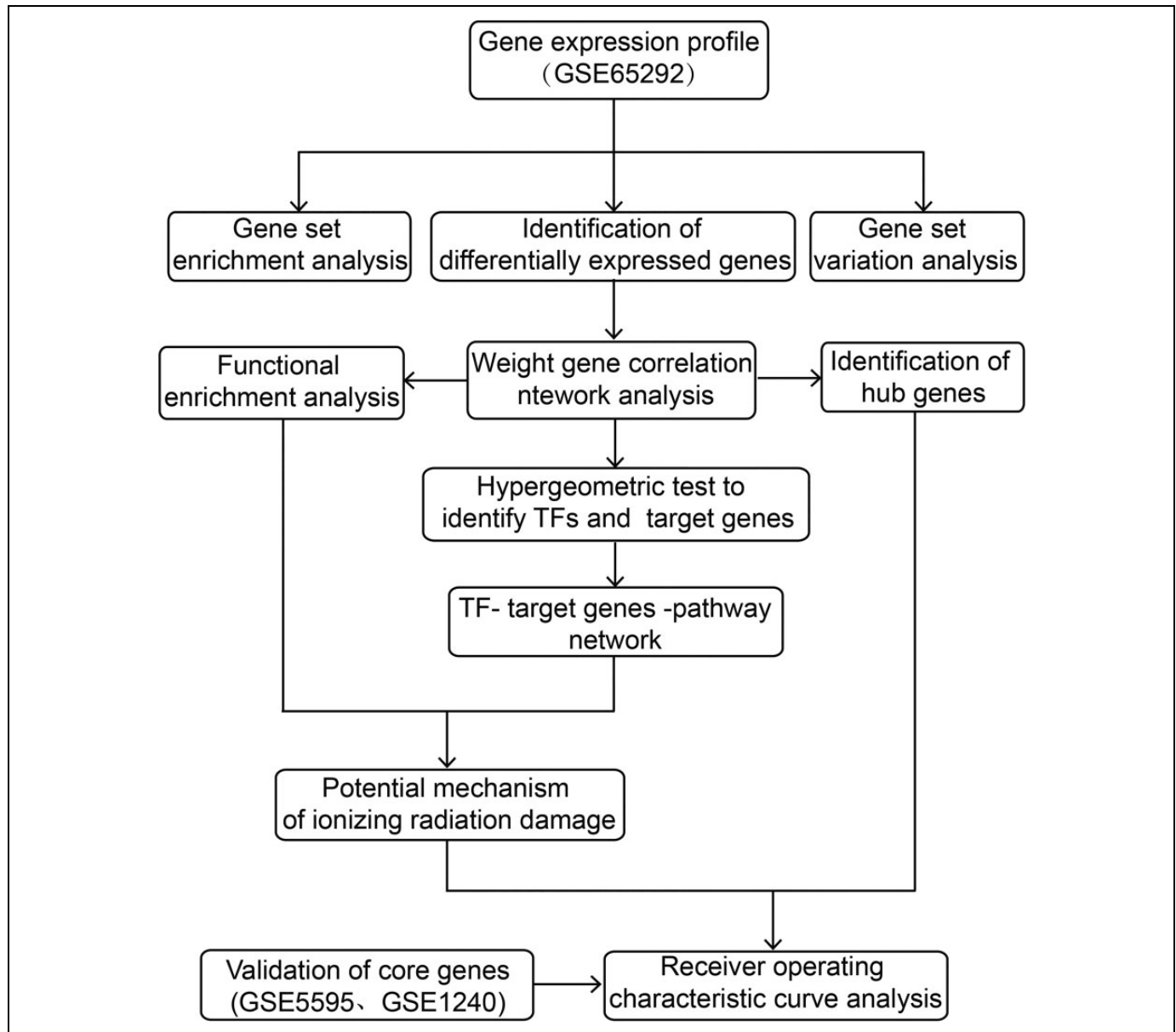


Figure 1. Flowchart of the present study.

considered significant. In addition, ClueGO²¹ in Cytoscape²² was used to perform BPs enrichment analysis for each module.

Hypergeometric Test and Correlation Analysis

In order to predict the upstream TFs of the regulatory modules, hypergeometric test was carried out. Interactions between TFs and their target genes were downloaded from TRRUST v2 database.²³ Interactions between a regulator and a related functional module were examined using the hypergeometric test in R. Interactions between a regulator and a functional module that showed quantity >2 and $P < 0.05$ were considered significant. Moreover, we analyzed Pearson correlation between a TF and each of its targets to reduce noise and false positives. A $P < 0.05$ was considered significant. Combining enrichment

analysis results, a TF-target genes-pathway network was constructed.

Hub Genes and Receiver Operating Characteristic Curve

In WGCNA, gene significance (GS) is defined as the correlation a gene with phenotype. The module membership (MM) is defined to measure the importance of a gene in the module. In this study, a gene with $GS > 0.8$ and $MM > 0.9$ was defined as a hub gene among the candidate modules. Then, the pROC package²⁴ was used to conduct the receiver operating characteristic (ROC) curve analysis for these hub genes and TF and their target genes. Molecules with area under ROC (AUC) > 0.9 were identified as the core genes of IR damage.

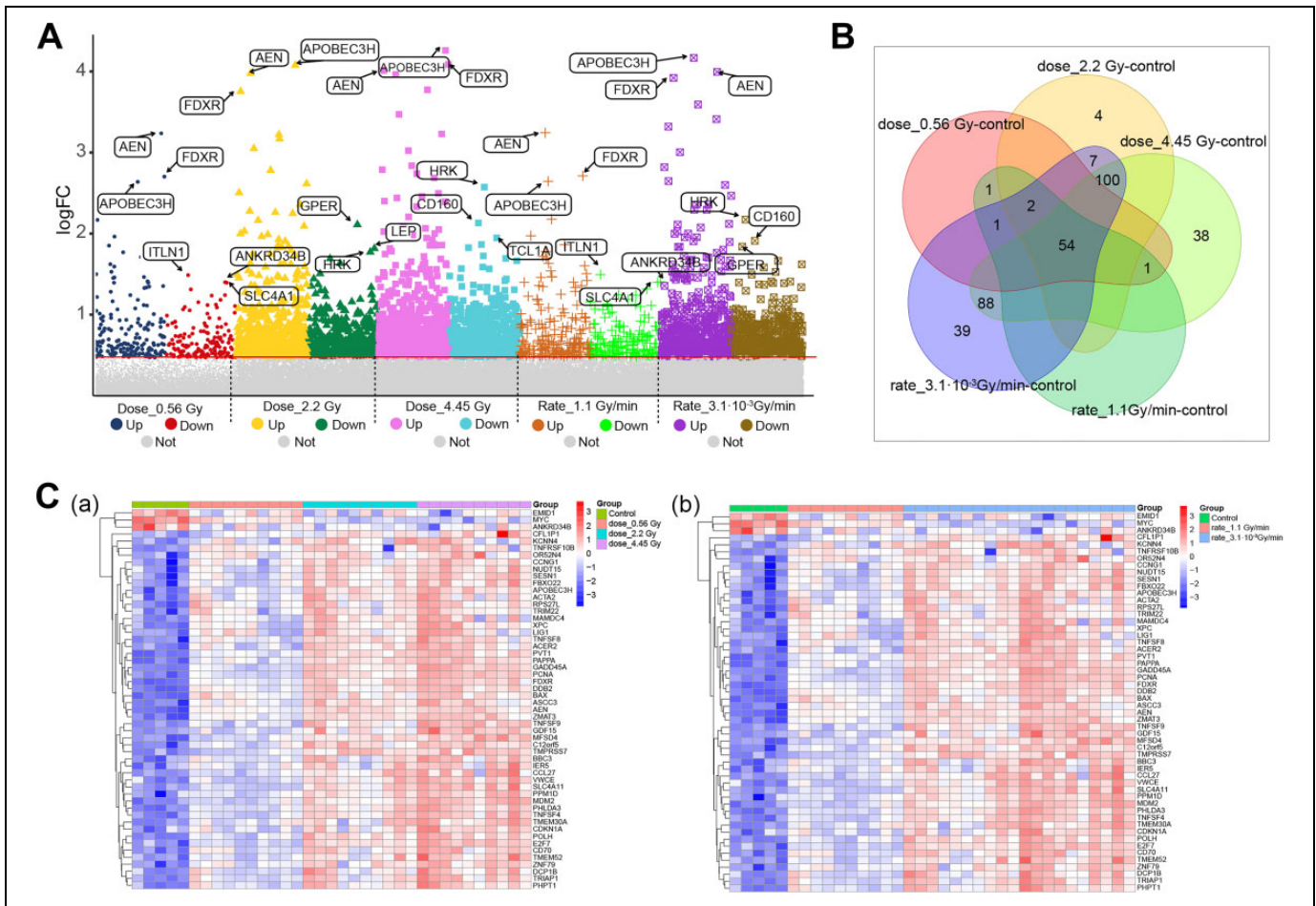


Figure 2. Differentially expressed gene (DEG) analysis. **A**, Manhattan plot for associations between different degree ionizing radiation damages and control, the first 3 genes with the highest significance were highlighted. **B**, Common DEGs in dose_0.56 Gy control, dose_2.2 Gy control, dose_4.45 Gy control, rate_1.1 Gy/min control, and rate_3.1 mGy/min control. **C**, (a) Heatmap of 54 common DEGs in different dose controls. (b) Heatmap of 54 common DEGs in different rate controls.

Result

Molecular Imbalance in Peripheral Blood Induced by Gradient Dose and Rate of Radiotherapy

Compared to control samples, there are 59 DEGs in 0.56 Gy dose, 3 of which were upregulated, 56 of which were down-regulated; 167 DEGs in 2.2 Gy dose, 52 of which were upregulated, 115 of which were downregulated; 281 DEGs in 4.45 Gy dose, 108 of which were upregulated, 173 of which were downregulated; 59 DEGs in 1.1 Gy/min, 5 of which were upregulated, 54 of which were downregulated; 291 DEGs in 3.1 mGy/min, 114 of which were upregulated, 177 of which were downregulated. The 3 genes with the highest significance (ranked by fold-change) in each comparison were visualized (Figure 2A), and these genes may be affected by radiation the most. We found 54 common DEGs in peripheral blood samples that received different radiation doses and rates (Figure 2B). They may be radiation-specific genes. In addition, the expressions of the

54 common DEGs can basically distinguish between different cases and controls (Figure 2C).

Synergistic Expressions of Disordered Molecules Were Observed and Significantly Correlated With Doses and Rates

In the WGCNA, power = 0.86 was estimated by the package (Figure 3A), and a total of 4 functional modules were identified (Figure 3B). Each module was given an individual color as its identifier. The colors are brown, blue, turquoise, and gray. The analysis showed that these functional modules were significantly correlated with the dose and the rate of acceptance of IR, of which the brown module is negatively correlated with the dose and rate of IR. The blue and the turquoise modules are positively correlated with the dose and rate of IR (Figure 3C). We also constructed a topological overlap matrix plot and found that the genes in all modules have strong coexpression relationships (Figure 3D).

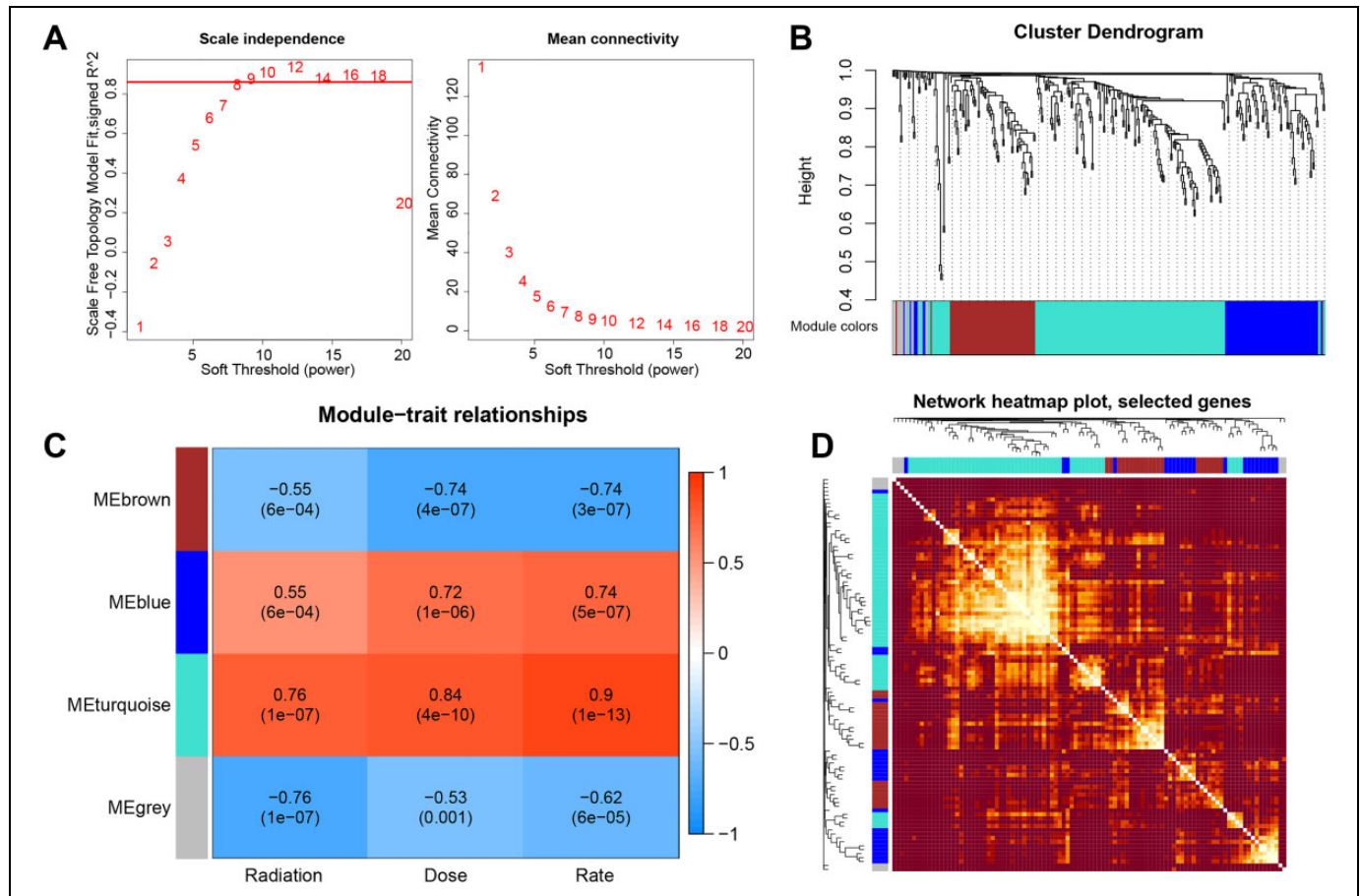


Figure 3. Weighted gene correlation analysis. A, Dynamic branch cutting. B, Hierarchical clustering, each color represents a functional module. C, Correlation heatmap of gene modules and phenotypes. Red indicates a positive correlation, and blue indicates a negative correlation. D, Topological overlap matrix (TOM) plot for the gene coexpression network of the intramodules. In the TOM plot, the light color indicates low topological overlap, while the darker color indicates high topological overlap.

Biological Processes and Pathways Involved in Dose- and Rate-Dependent Modules

To study the underlying biological functions of these modules, functional enrichment analysis was carried out. The results of GO analysis (Figure 4A) revealed that genes in the blue module were significantly involved in entry into host cells, entry into hosts, entry into other organism involved in symbiotic interaction, and entry into cell of other organisms involved in symbiotic interaction. Genes in the brown module were significantly involved in B-cell proliferation, B-cell activation, and dendrite extension. Genes in the turquoise module were significantly involved in signal transduction in response to DNA damage, DDR, and signal transduction by p53 class mediator. An analysis of the KEGG pathway (Figure 4B) showed that the blue module was significantly involved in natural killer cell-mediated cytotoxicity and FoxO signaling pathway, the brown module was significantly involved in PI3K-Akt signaling pathway, and the turquoise module was significantly involved in p53 signaling pathway, necroptosis, human papillomavirus infection, apoptosis, and alcoholism. In addition, Clue Go analysis indicates (Figure 4C) that the brown module was involved in deoxyribonucleotide metabolic process,

muscle cell cellular homeostasis, and dendrite extension; the blue module was involved in negative regulation of cell-matrix adhesion; and the turquoise module was involved in signal transduction by p53 class mediator, response to UV cellular, response to UV, and DNA cytosine deamination. Moreover, the GSEA results indicated that apoptosis pathway was significantly enriched in the samples of 0.56 Gy dose, 2.2 Gy dose, and 1.1 Gy/min rate, and p53 signaling pathway was significantly enriched in samples of 0.56 Gy dose, 2.2 Gy dose, 4.45 Gy dose, 1.1 Gy/min rate; and 3.1 mGy/min rate (Figure 4D). The GSEA results indicated the gene set variations in both apoptosis and p53 signaling pathway were gradually increased with the increase in dose and rate (Figure 4E).

Potential Mechanism of IR Damage

Hypergeometric test result showed that in the turquoise module, 3 TFs (ESR1, ATM, and MYC; Table S1) were significantly correlated with 6 target genes (*TNFRSF10B*, *MDM2*, *CDKN1A*, *FAS* [also known as *TNFRSF6*], *PCNA*, and *GADD45A*; Figure 5A). Therefore, a TF-target genes-pathway global regulatory network was constructed (Figure 5B). According to gene differential expression analysis, most

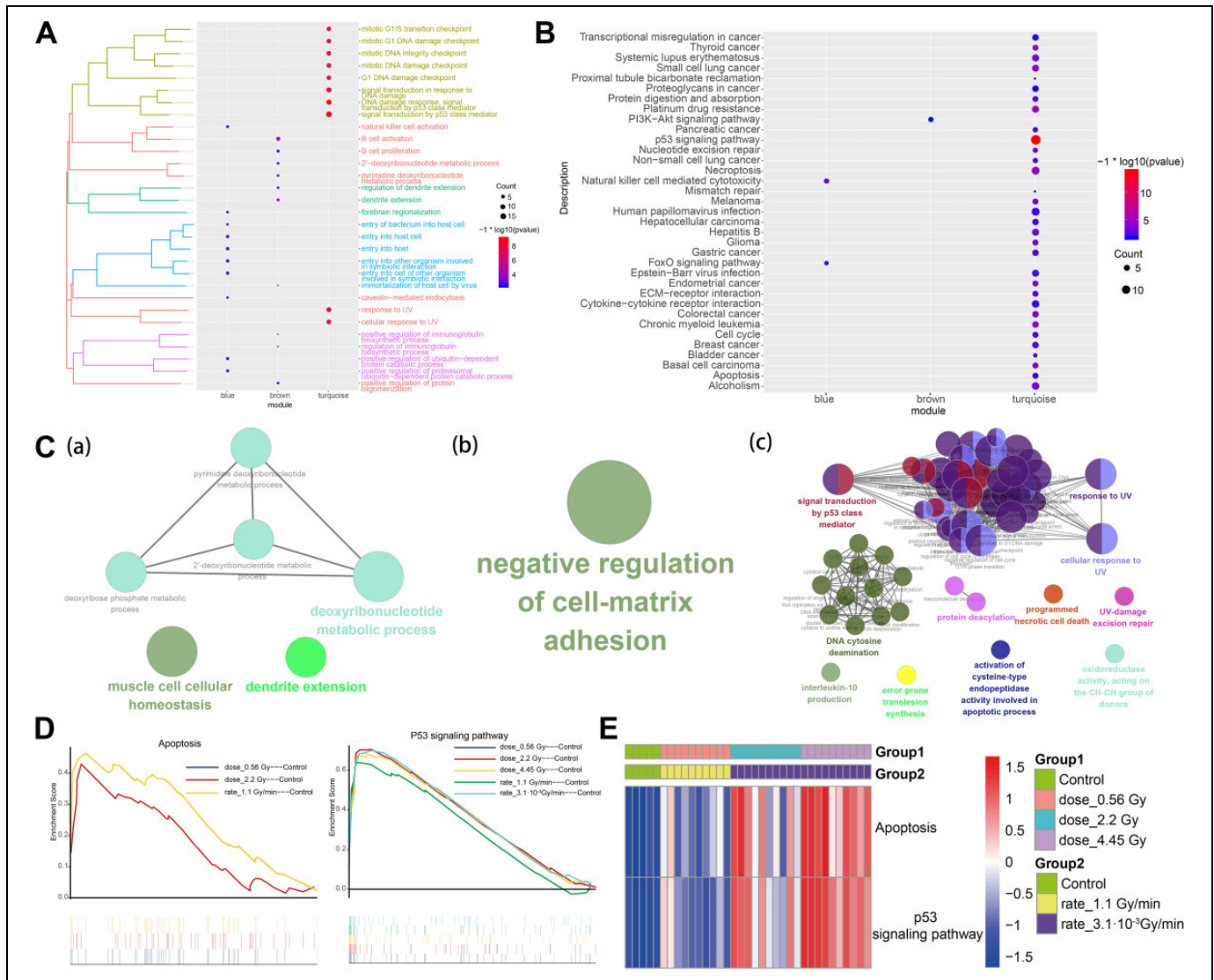


Figure 4. Biological processes and Kyoto Encyclopedia of Genes and Genomes (KEGG) pathways enrichment analysis of functional modules. A, Biological processes of functional modules, similar biological processes were clustered. B, KEGG pathways of functional modules. C, Biological processes of functional modules in Clue Gene Ontology. D, Apoptosis and P53 signaling pathway were enriched in different samples. In apoptosis, the lines of 0.56 Gy and 1.1 Gy/min were overlapping. E, The gene set variations of both apoptosis and p53 signaling pathway were gradually increased with the increase of dose and rate.

DEGs regulated by TF in apoptosis and p53 signaling pathway show high expressions, and the expressions of DEGs increased with the increase in radiation dose and rate. These may be relevant to the degree of IR damage, which has been confirmed in GSEA. Thus, apoptosis and p53 signaling pathway were identified as the potential mechanism of RIBE and IR damage (Figure 5C).

Core Molecules of Gradient Dose- and Rate-Radiation Damage

Furthermore, according to $GS > 0.8$ and $MM > 0.9$, 14 genes were identified as hub genes (*PHLDA3*, *GADD45A*,

PCNA, *TNFSF4*, *MDM2*, *E2F7*, *VWCE*, *FHL2*, *DRAM1*, *FDXR*, *DDB2*, *PVT1*, *ZMAT3*, and *PAPPA*). Therefore, ROC curve analyses were performed on hub genes, TF of participation mechanism, and TF target genes. The result suggested that 13 genes have a strong ability to distinguish whether or not it was exposed to IR and were identified as core genes (Figure 6A), which were further validated in GSE55953 (Figure 6B) and GSE21240 (Figure 6C). In addition, it was found by comparing with the controls, the expressions of these genes were gradually upregulated with the increase in rate and dose in IR sample (Figure 7A), and these aberrant expressions were validated by GSE55953 (Figure 7B) and GSE21240 (Figure 7C).

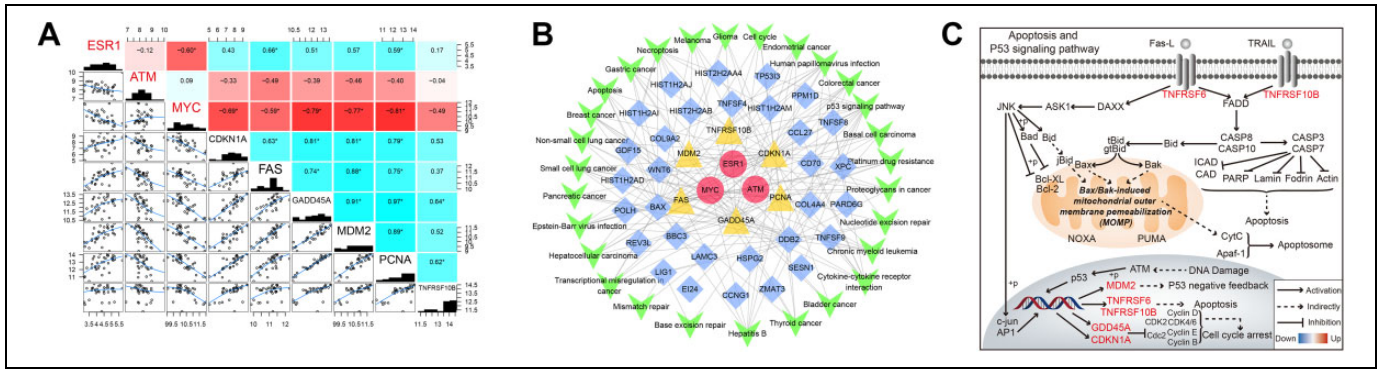


Figure 5. Potential mechanism of IR damage. A, The correlation between TFs and its target genes. B, TF-target genes pathway network. C, Potential mechanism of IR damage. Red genes represent the target genes of TFs (ATM, ESR1, and MYC). IR indicates ionizing radiation; TF, transcription factor.

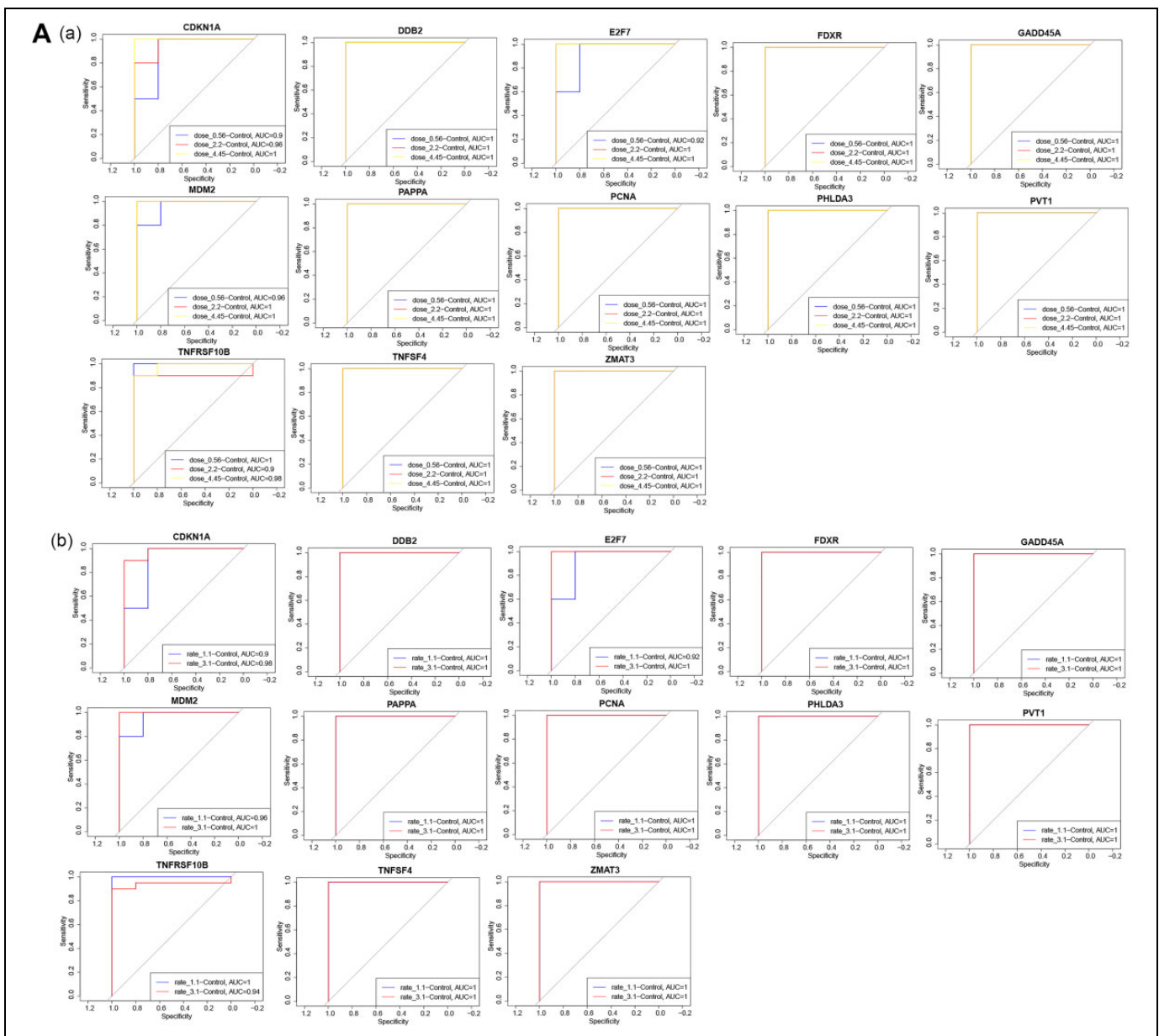


Figure 6. Identification of core molecules in ionizing radiation damage. A, (a) Receiver operating characteristic (ROC) curve analysis of core molecules by doses. (b) ROC curve analysis of core molecules by rates. B, ROC curve analysis of core molecules in GSE55953. C, ROC curve analysis of core molecules in GSE21240.

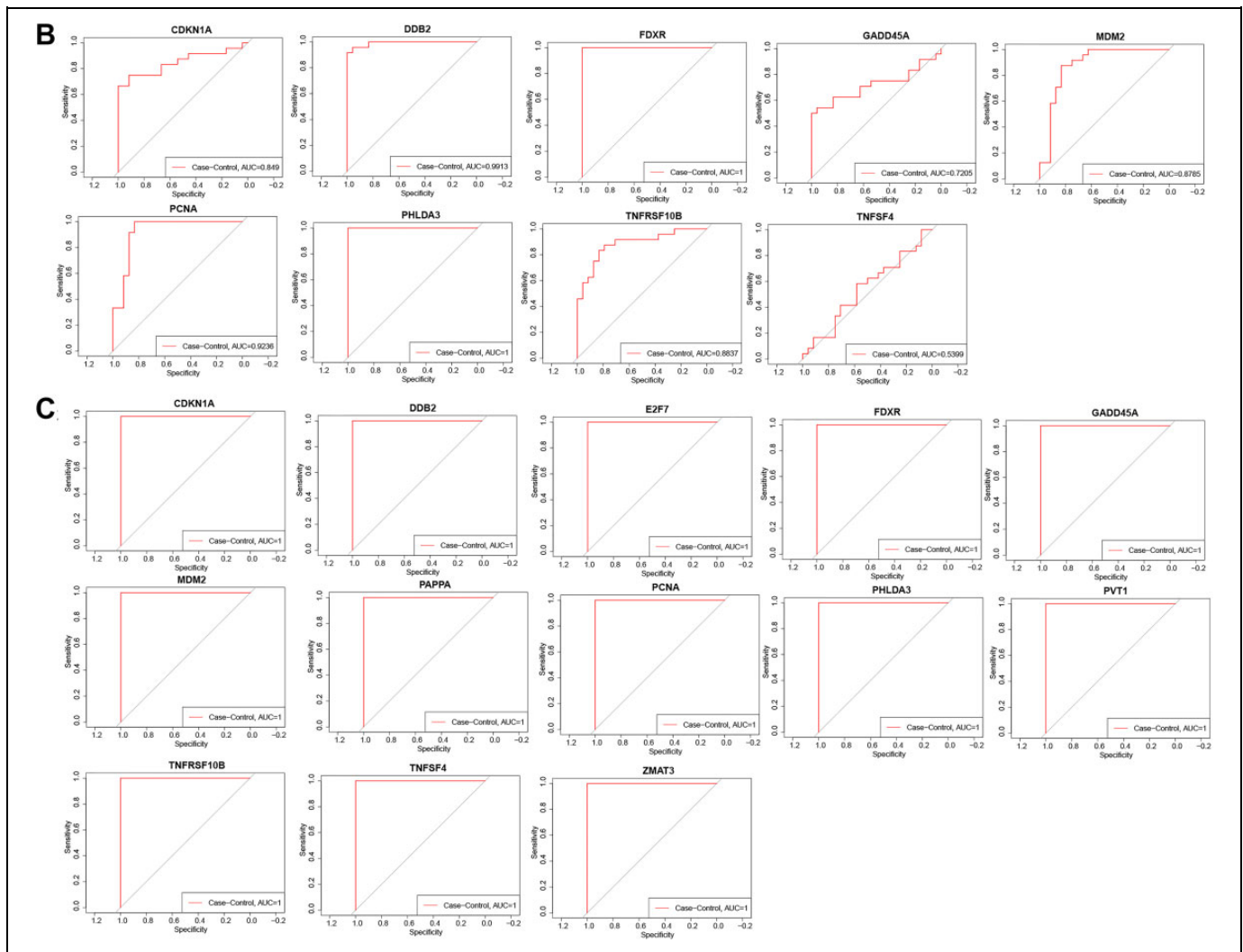


Figure 6. (Continued).

Discussion

Although radiotherapy is a local treatment, the body's response to radiotherapy is systematic. There are no circulating biomarkers for measuring this systemic response. In our current study, we sought to explore whether this systemic response is reflected in the peripheral blood transcriptome. Radiation-induced bystander effect is one of the systemic responses of the body to radiotherapy. When subjected to radiation therapy, adjacent tissues are inevitably affected by radiation, which may produce RIBE. RIBE refers to the process in which factors released by irradiated cells or tissues affect other parts of nonirradiated parts of the body animals, leading to genomic instability, stress response, and changes in apoptosis or cell proliferation.^{4,25,26} Existing literatures indicated that RIBE may be mediated directly by gap junction intercellular communication and/or divergent cellular factors increased from irradiated cells.²⁷⁻²⁹ However, it has also been indicated in literatures that gap junction inhibitors or enhancers had no

effect on the bystander effect of human lung cancer cell lines or rat tumor cell lines.³⁰ Therefore, more study on potential of mechanism of RIBE are necessary. To further explore these important issues in radiotherapy, we carried out a comprehensive analysis of peripheral blood samples irradiated at different doses and rates in this study. We found that the DEGs of samples irradiated by different doses and rates are different. Our WGCNA result identified 4 functional modules, which have similar statistical significances on dose and rate dependence. These modules have different correlations with radiation dose and rate, indicating they may perform different functions in the body's response to radiation. Among them, the coexpression of gray module genes was not significant, and the coexpression of the other 3 modules were significant. Among these 3, the blue module genes were mainly involved in functions such as entry into hosts, the brown module genes were mainly involved in functions such as activation and differentiation of immune cells, and the turquoise module genes are mainly involved in functions

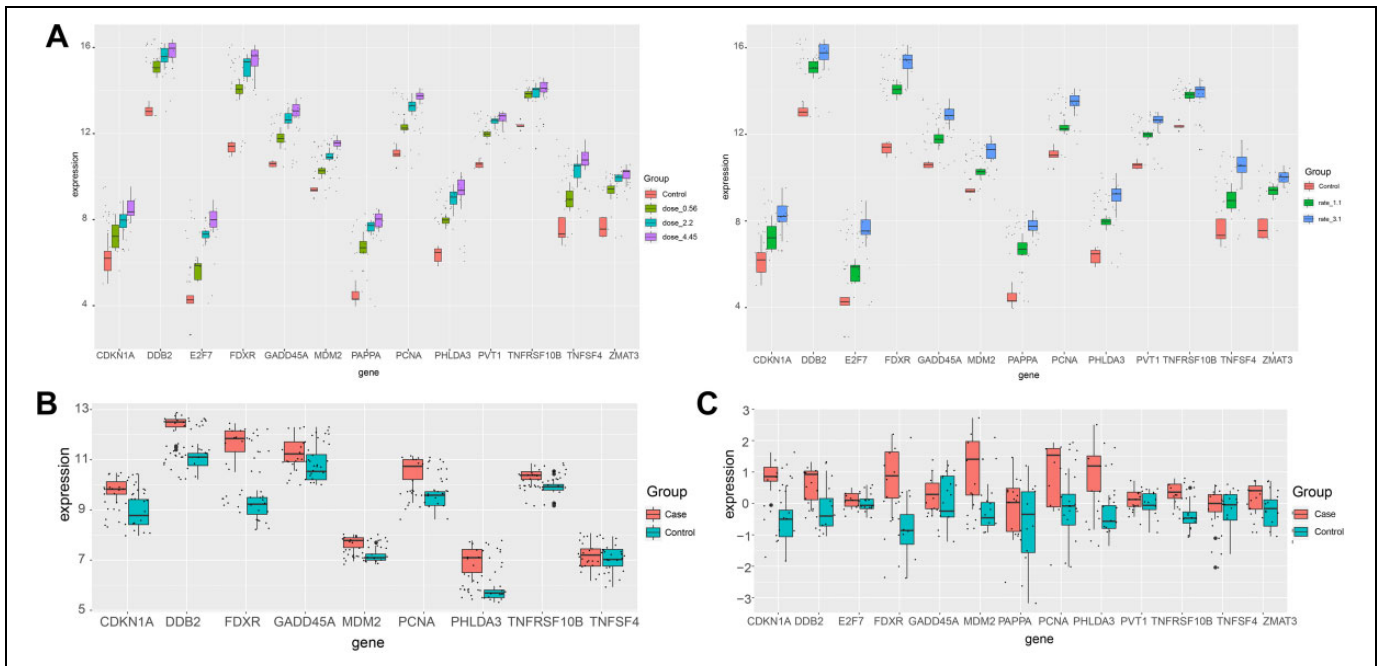


Figure 7. Trends of gene expressions in different samples. A, Core molecules were gradually upregulated in different doses ionizing radiation (IR) damages and were gradually upregulated in different rate IR damages. B, Core molecules were upregulated in IR damage of GSE55953. C, Core molecules were upregulated in IR damage of GSE1240.

such as DNA damage checkpoints. Moreover, our functional enrichment analysis indicated that the functional modules were significantly involved in natural killer cell-mediated cytotoxicity, PI3K-Akt signaling pathway, p53 signaling pathway, and apoptosis. The GSEA showed p53 signaling pathway and apoptosis were also enriched in most radiated samples, suggesting that apoptosis and p53 signaling pathway may be the major potential mechanisms of IR damage. The major consequence of IR exposure is the generation of single- or double-stranded breaks in DNA, which result in DNA damage,^{31,32} thus elicited a cellular stress response that includes DNA damage recognition and cell-cycle arrest, followed by DNA repair or apoptosis.³³ In addition, the radiated blood in the capillaries of the radiotherapy site circulates throughout the body, which may contribute to the formation of RIBE. These are supportive of our finding that apoptosis and p53 signaling pathway may be the major factor of RIBE.

In addition, 3 TFs (ESR1, ATM, and MYC) and their target genes (*TNFRSF10B*, *MDM2*, *CDKN1A*, *FAS*, *PCNA*, and *GADD45A*) were identified, and a TF-target genes pathway global regulatory network was constructed based on the hypergeometric test. Existing studies indicated that MYC was required for activation of the ATM-dependent checkpoints in response to DNA damage,³⁴ and the kinase activity of cells of ATM can be activated by IR irradiation.^{35,36} Moreover, it was also confirmed that the N-terminal of ATM and ATM's kinase activity were required for activation of p53's transcriptional activity and restoration of normal sensitivity to DNA damage.³⁷ Furthermore, 6 TF target genes are involved in a variety

of pathways, including DNA repair (*PCNA*), cell-cycle progression (*CDKN1A* and *GADD45A*), and cell death (*TNFRSF10B* and *TNFRSF6*).³⁸ It was also reported in the literature that DNA damage induced by IR involved P53 protein disorders. The increase in p53 protein levels thus can lead to the induction of many genes, including *ACTA2*, *CDKN1A*, *DDB2*, *FDXR*, *GADD45A*, *PIG3*, *TNFRSF6*, and *TNFSF10B*.³⁹⁻⁴² The upregulation of these genes leads to a diverse set of events, including cell-cycle arrest, DNA repair, and apoptosis. These results of the existing studies are supportive to our founding.

Moreover, we identified 13 core molecules of IR damage: *CDKN1A*, *DDB2*, *E2F7*, *FDXR*, *GADD45A*, *MDM2*, *PAPP*, *PCNA*, *PHLDA3*, *PVT1*, *TNFRSF10B*, *TNFSF4*, and *ZMAT3*. They were also upregulated in IR samples compared to controls, and most of them were involved in the p53 signaling pathway.^{38,43} Among them, *CDKN1A*, *DDB2*, *FDXR*, *GADD45A*, *PCNA*, and *TNFRSF10B* are known radiation-response genes, which have a sustained radiation dose-response and a strong positive correlation with dose.⁴⁴ Therefore, these genes may be part of the main circulating biomarkers of IR damage. If this is confirmed, it will be able to help us identify and understand IR-related risks associated with radiological examinations and radiotherapy. We plan to further verify our findings using experiments.

Conclusion

This study showed apoptosis and ATM-p53 signaling pathway, and ESR1, ATM, and MYC may be mainly responsible for radiotherapy damage to human body. Thus, understanding their

roles in the related transcription regulatory network may help us understand the biological mechanism of radiotherapy damage.

Authors' Note

G.H., A.T., and M.X. contributed equally to this work.

Acknowledgments

The authors thank the Life-Ontology Biological Technology Co, Ltd, for assisting with bioinformatics analysis.


Declaration of Conflicting Interests

The author(s) declared no potential conflicts of interest with respect to the research, authorship, and/or publication of this article.

Funding

The author(s) disclosed receipt of the following financial support for the research, authorship, and/or publication of this article: This study was supported by the National Natural Science Foundation of China (grant no. 81760189), Guangxi Education Department of China (grant no. KY2016YB094), and Guangxi Scholarship Fund of Guangxi Education Department of China. Y.M.Z. was supported by a Simons Foundation Collaboration Grant for Mathematicians (416937).

ORCID iD

Yi Ming Zou  <https://orcid.org/0000-0001-7471-5971>

Supplemental Material

Supplemental material for this article is available online.

References

- Thariat J, Hannoun-Levi JM, Sun Myint A, Vuong T, Gerard JP. Past, present, and future of radiotherapy for the benefit of patients. *Nat Rev Clin Oncol*. 2013;10(1):52-60.
- Baskar R, Lee KA, Yeo R, Yeoh KW. Cancer and radiation therapy: current advances and future directions. *Int J Med Sci*. 2012;9(3):193-199.
- Chaudhry MA. Bystander effect: biological endpoints and microarray analysis. *Mutat Res*. 2006;597(1-2):98-112.
- Rzeszowska-Wolny J, Przybyszewski WM, Widel M. Ionizing radiation-induced bystander effects, potential targets for modulation of radiotherapy. *Eur J Pharmacol*. 2009;625(1-3):156-164.
- Hamada N, Maeda M, Otsuka K, Tomita M. Signaling pathways underpinning the manifestations of ionizing radiation-induced bystander effects. *Curr Mol Pharmacol*. 2011;4(2):79-95.
- Widel M, Przybyszewski W, Rzeszowska-Wolny J. Radiation-induced bystander effect: the important part of ionizing radiation response. Potential clinical implications [in Polish]. *Postepy Hig Med Dosw (Online)*. 2009;63:377-388.
- Klammer H, Mladenov E, Li F, Iliakis G. Bystander effects as manifestation of intercellular communication of DNA damage and of the cellular oxidative status. *Cancer Lett*. 2015;356(1):58-71.
- Paul S, Amundson SA. Development of gene expression signatures for practical radiation biodosimetry. *Int J Radiat Oncol Biol Phys*. 2008;71(4):1236-1244.
- Amundson SA, Do KT, Shahab S, et al. Identification of potential mRNA biomarkers in peripheral blood lymphocytes for human exposure to ionizing radiation. *Radiat Res*. 2000;154(3):342-346.
- Boldt S, Knops K, Kriehuber R, Wolkenhauer O. A frequency-based gene selection method to identify robust biomarkers for radiation dose prediction. *Int J Radiat Biol*. 2012;88(3):267-276.
- Dressman HK, Muramoto GG, Chao NJ, et al. Gene expression signatures that predict radiation exposure in mice and humans. *PLoS Med*. 2007;4(4):e106.
- Ghandhi SA, Smilenov LB, Elliston CD, Chowdhury M, Amundson SA. Radiation dose-rate effects on gene expression for human biodosimetry. *BMC Med Genomics*. 2015;8:22.
- Barrett T, Wilhite SE, Ledoux P, et al. NCBI GEO: archive for functional genomics data sets—update. *Nucleic Acids Res*. 2013;41(Database issue):D991-D995.
- Beer L, Zimmermann M, Mitterbauer A, et al. Analysis of the secretome of apoptotic peripheral blood mononuclear cells: impact of released proteins and exosomes for tissue regeneration. *Sci Rep*. 2015;5:16662.
- Beer L, Seemann R, Ristl R, et al. High dose ionizing radiation regulates micro RNA and gene expression changes in human peripheral blood mononuclear cells. *BMC Genomics*. 2014;15(1):814.
- Ritchie ME, Phipson B, Wu D, et al. Limma powers differential expression analyses for RNA-sequencing and microarray studies. *Nucleic Acids Res*. 2015;43(7):e47.
- Liberzon A, Birger C, Thorvaldsdottir H, Ghandi M, Mesirov JP, Tamayo P. The Molecular Signatures Database (MSigDB) hallmark gene set collection. *Cell Syst*. 2015;1(6):417-425.
- Hanzelmann S, Castelo R, Guinney J. GSEA: gene set variation analysis for microarray and RNA-seq data. *BMC Bioinformatics*. 2013;14:7.
- Langfelder P, Horvath S. WGCNA: an R package for weighted correlation network analysis. *BMC Bioinformatics*. 2008;9:559.
- Yu G, Wang LG, Han Y, He QY. clusterProfiler: an R package for comparing biological themes among gene clusters. *OMICS*. 2012;16(5):284-287.
- Bindea G, Mlecnik B, Hackl H, et al. ClueGO: a Cytoscape plugin to decipher functionally grouped Gene Ontology and pathway annotation networks. *Bioinformatics*. 2009;25(8):1091-1093.
- Shannon P, Markiel A, Ozier O, et al. Cytoscape: a software environment for integrated models of biomolecular interaction networks. *Genome Res*. 2003;13(11):2498-2504.
- Han H, Cho JW, Lee S, et al. TRRUST v2: an expanded reference database of human and mouse transcriptional regulatory interactions. *Nucleic Acids Res*. 2018;46(D1):D380-D386.
- Robin X, Turck N, Hainard A, et al. pROC: an open-source package for R and S+ to analyze and compare ROC curves. *BMC Bioinformatics*. 2011;12:77.
- Prise KM, O'Sullivan JM. Radiation-induced bystander signalling in cancer therapy. *Nat Rev Cancer*. 2009;9(5):351-360.
- Mothersill C, Seymour C. Radiation-induced bystander effects: past history and future directions. *Radiat Res*. 2001;155(6):759-767.
- Shao C, Furusawa Y, Aoki M, Ando K. Role of gap junctional intercellular communication in radiation-induced bystander effects in human fibroblasts. *Radiat Res*. 2003;160(3):318-323.

28. Bishayee A, Hill HZ, Stein D, Rao DV, Howell RW. Free radical-initiated and gap junction-mediated bystander effect due to nonuniform distribution of incorporated radioactivity in a three-dimensional tissue culture model. *Radiat Res.* 2001;155(2):335-344.
29. Azzam EI, de Toledo SM, Little JB. Direct evidence for the participation of gap junction-mediated intercellular communication in the transmission of damage signals from alpha-particle irradiated to nonirradiated cells. *Proc Natl Acad Sci U S A.* 2001;98(2):473-478.
30. Imaizumi K, Hasegawa Y, Kawabe T, et al. Bystander tumoricidal effect and gap junctional communication in lung cancer cell lines. *Am J Respir Cell Mol Biol.* 1998;18(2):205-212.
31. Hutchinson F. Chemical changes induced in DNA by ionizing radiation. *Prog Nucleic Acid Res Mol Biol.* 1985;32:115-154.
32. Ward JF. DNA damage produced by ionizing radiation in mammalian cells: identities, mechanisms of formation, and reparability. *Prog Nucleic Acid Res Mol Biol.* 1988;35:95-125.
33. Jen KY, Cheung VG. Transcriptional response of lymphoblastoid cells to ionizing radiation. *Genome Res.* 2003;13(9):2092-2100.
34. Guerra L, Albiñ A, Tronnersjo S, et al. Myc is required for activation of the ATM-dependent checkpoints in response to DNA damage. *PLoS One.* 2010;5(1):e8924.
35. Bakkenist CJ, Kastan MB. DNA damage activates ATM through intermolecular autophosphorylation and dimer dissociation. *Nature.* 2003;421(6922):499-506.
36. Kozlov SV, Graham ME, Peng C, Chen P, Robinson PJ, Lavin MF. Involvement of novel autophosphorylation sites in ATM activation. *EMBO J.* 2006;25(15):3504-3514.
37. Turenne GA, Paul P, Laflair L, Price BD. Activation of p53 transcriptional activity requires ATM's kinase domain and multiple N-terminal serine residues of p53. *Oncogene.* 2001;20(37):5100-5110.
38. Rashi-Elkeles S, Elkon R, Shavit S, et al. Transcriptional modulation induced by ionizing radiation: p53 remains a central player. *Mol Oncol.* 2011;5(4):336-348.
39. Amundson SA, Bittner M, Chen Y, Trent J, Meltzer P, Fornace AJ Jr. Fluorescent cDNA microarray hybridization reveals complexity and heterogeneity of cellular genotoxic stress responses. *Oncogene.* 1999;18(24):3666-3672.
40. Zhao R, Gish K, Murphy M, et al. Analysis of p53-regulated gene expression patterns using oligonucleotide arrays. *Genes Dev.* 2000;14(8):981-993.
41. Kannan K, Amariglio N, Rechavi G, et al. DNA microarrays identification of primary and secondary target genes regulated by p53. *Oncogene.* 2001;20(18):2225-2234.
42. Tusher VG, Tibshirani R, Chu G. Significance analysis of microarrays applied to the ionizing radiation response. *Proc Natl Acad Sci U S A.* 2001;98(9):5116-5121.
43. el-Deiry WS. Regulation of p53 downstream genes. *Semin Cancer Biol.* 1998;8(5):345-357.
44. Ghandhi SA, Shuryak I, Morton SR, Amundson SA, Brenner DJ. New approaches for quantitative reconstruction of radiation dose in human blood cells. *Sci Rep.* 2019;9(1):18441.